with benzenoid rings are more important than structures with quininoid rings. It is of interest to test the application of this rule to some of the structures and its effect on the bond-length predictions.

In the case of pyrene, two of the six structures each have three benzenoid rings, two have two benzenoid rings, and two have only one. If the contributions of these structures to the normal state are weighted in proportion to their benzenoid character, the most important effect is to increase the length of the central bond in Fig. 4 to 1·46 A., in good agreement with the observations. The four inner bonds adjacent to it become 1·40 A. instead of 1·42 A., while the other four long bonds on the outer edge become 1·50 A. instead of 1·46 A. The general effect is thus to make some qualitative improvement in the predicted bond lengths.

When the dibenzanthracene structures are treated in the same way the effect is disappointing. The predicted bond lengths in the central ring become equalized at the benzene value of 1·39 A., while in other parts of the molecule the values obtained are more extreme than those shown in Fig. 9 and not in any better agreement with the observations.

Of the twenty coronene structures, one contains five benzenoid rings, eight contain four benzenoid rings, six contain three benzenoid rings, three contain two benzenoid rings and two contain only one benzenoid ring. Weighting the contributions of the structures according to these benzenoid characters has little effect on the dimensions given in Fig. 13. Rather more extreme values are obtained for the bond-length variations, but the general picture is the same. In particular it may be noted that no combination of the Kekulé structures is capable of differentiating the longer bonds of the outer ring from the bonds of the inner ring.

The general impression based on our very limited data is that application of the Fries rule tends to improve the agreements slightly, and this finding is in accordance with chemical experience as well as theoretical expectation.

Figs. 2, 6 and 11 are reproduced by kind permission from the *Journal of the Chemical Society*.

References

COULSON, R. A. (1944). *Nature, Lond.*, **154**, 797.

DAUDEL, R. & PULLMAN, A. (1946). *J. Phys. Radium*, **59**, 74.

IBALL, J. (1936). *Nature, Lond.*, **137**, 361.

IBALL, J. & ROBERTSON, J. M. (1933). *Nature, Lond.*, **132**, 750.

KRISHNAN, K. S. & BANERJEE, S. (1935). *Z. Krystallogr.* **91**, 170.

PAULING, L. (1939). *The Nature of the Chemical Bond.* Cornell: University Press.

PAULING, L. & BROCKWAY, L. O. (1937). *J. Amer. Chem. Soc.* **59**, 1223.

ROBERTSON, J. M. (1933*a*). *Proc. Roy. Soc.* A, **140**, 79.

ROBERTSON, J. M. (1933*b*). *Proc. Roy. Soc.* A, **142**, 674.

ROBERTSON, J. M. & WHITE, J. G. (1945). *J. Chem. Soc.* p. 607.

ROBERTSON, J. M. & WHITE, J. G. (1947*a*). *Proc. Roy. Soc.* A, **190**, 329.

ROBERTSON, J. M. & WHITE, J. G. (1947*b*). *J. Chem. Soc.* p. 358.

ROBERTSON, J. M. & WHITE, J. G. (1947*c*). *J. Chem. Soc.* p. 1001.

ROBERTSON, J. M. & WHITE, J. G. (in the Press). *J. Chem. Soc.*

VOLLMANN, H., BECKER, H., CORELL, M., STREECK, H. & LANGBEIN, G. (1937). *Liebigs Ann.* **531**, 1.

WHITE, J. G. (in the Press). *J. Chem. Soc.*

Acta Cryst. (1948). **1**, 109

Indexing Method of Powder Photographs of Long-Spacing Compounds

BY VLADIMIR VAND

Research Laboratories, Lever Brothers and Unilever Limited, Port Sunlight, Cheshire, England

(*Received* 7 *November* 1947 *and in revised form* 13 *January* 1948)

A method suitable for indexing X-ray powder photographs of compounds which give long-spacing reflexions is described. The method reduces the problem to that of a two-dimensional lattice. As an example, the unit cell of potassium caproate is deduced from its powder pattern by means of two graphical variants of the method. Limitations of the method are discussed.

Introduction

Crystal structure study of many long-chain substances, such as certain forms of soaps, fats and fatty acids, is considerably hampered by the difficulty of growing single crystals large enough for a complete X-ray diffraction analysis. However, a considerable amount of information can be obtained from powder photographs and from other properties of the long-chain compounds, provided the 'long spacings' can be measured. This is due to certain characteristic peculiarities of their crystals, which reduce the three-dimensional problem of the determination of their crystal lattice to a simpler

two-dimensional problem within a single sheet or layer of the space lattice, and, although the information gained may not be as complete as that obtained from single-crystal work, it may prove to be of considerable value.

We shall discuss only those compounds whose long spacings can be unambiguously identified from powder photographs. These compounds may be called 'long-spacing compounds', in order to distinguish them from 'long-chain compounds', such as polymers, which do not necessarily give identifiable long-spacing reflexions.

Long-spacing compounds usually crystallize in very thin plates, the only developed faces being {001}. Occasionally they crystallize in needles, but these can be regarded as derived from plates by faster growth along one of the short axes; the rod-like molecules as a rule then do not lie along the needle axis, but rather perpendicular or at an angle to the needle axis. In this respect, they differ from the long-chain polymer fibres, which usually have molecules oriented along the fibre axis.

Theory of the indexing method

In a powder photograph, the crystal spacings d/n are given by

$$d/n = \lambda/2 \sin \theta. \tag{1}$$

Their reciprocals, $n/d = D^*_{hkl}$, are the distances of the points having Miller indices h, k, l, from the origin of the reciprocal lattice. (All quantities referring to reciprocal space or reciprocal lattice will be marked with an asterisk, *.)

In order to index a triclinic crystal we have to find six unknown parameters, the edges a^*, b^*, c^* and the angles $\alpha^*, \beta^*, \gamma^*$ of the reciprocal unit cell, from a large number of equations of the form:

$$\left.\begin{aligned} D^{*2}_{hkl} = h^2a^{*2} + k^2b^{*2} + l^2c^{*2} + 2klb^*c^* \cos \alpha^* \\ + 2lhc^*a^* \cos \beta^* + 2hka^*b^* \cos \gamma^* \end{aligned}\right\}, \tag{2}$$

where h, k, l, are whole numbers, also unknown.

The problem is further complicated by missing reflexions due to the unknown space group absences, so that in practice the indexing of powder photographs can be successfully attempted only when the number of unknown parameters is small. The indexing methods hitherto used were successfully applied only to crystals of high symmetry, such as cubic, orthorhombic, tetragonal and hexagonal.

As the triclinic crystal involves six parameters, it appears that the task of indexing a powder photograph is very difficult. However, for crystals exhibiting long spacings, considerable simplifications bring the number of unknowns to be determined simultaneously from six down to three or even two, thus bringing the general problem of a triclinic crystal within practical reach of solution.

By a simple rearrangement of the terms, we can write equation (2) as follows:

$$\left.\begin{aligned} D^{*2}_{hkl} = h^2a^{*2} \sin^2 \beta^* + k^2b^{*2} \sin^2 \alpha^* \\ - 2ha^* \sin \beta^* \times kb^* \sin \alpha^* \frac{\cos \alpha^* \cos \beta^* - \cos \gamma^*}{\sin \alpha^* \sin \beta^*} \\ + (lc^* + ha^* \cos \beta^* + kb^* \cos \alpha^*)^2 \end{aligned}\right\} \tag{3}$$

As $$\frac{\cos \alpha^* \cos \beta^* - \cos \gamma^*}{\sin \alpha^* \sin \beta^*} = \cos \gamma,$$

we can write equation (3) in the form:

$$D^{*2}_{hkl} = H^{*2}_{hk} + L^{*2}_{hkl}, \tag{4}$$

where the following notation is used:

$$H^{*2}_{hk} = h^2A^{*2} + k^2B^{*2} - 2hkA^*B^* \cos \gamma, \tag{5}$$

$$L^*_{hkl} = lc^* + hA^* \cot \beta^* + kB^* \cot \alpha^*, \tag{6}$$

where $$A^* = a^* \sin \beta^*,$$

$$B^* = b^* \sin \alpha^*. \tag{7}$$

For crystals with long spacings c^* is much smaller than a^* and b^*. In equation (4), c^* does not appear in H^*, and the values of H^* represent a two-dimensional reciprocal lattice given by equation (5), having relatively large cell edges. On the other hand, the value of L^* is a linear function of l, and on variation of l it changes by much smaller steps than the variation of H^* when h and k are varied, as c^* is small. For certain values of l, it can also attain a small value, so that L^{*2}, although, in the general case of no symmetry, always positive, can approach rather closely zero, or even attain zero in special cases of higher crystal symmetry.

Equation (4) can thus be easily visualized: the powder diffraction pattern of a long-spacing compound is composed of a large number of bands of closely spaced lines, each band comprising all lines having the same values of h and k, and beginning with a crowded 'head' whose distance from the origin in reciprocal space is equal to H^*; however, at the head of the band need be neither $(hk0)$ nor the most intense line. As the chain length of the molecules increases, the value of c^* decreases, and the lines in each band are more crowded. As the values of H^* are independent of c^*, they are invariant for a series of substances all in the same modification, differing in long spacing only.

If the resolving power of a powder camera were sufficient and the background absent, so that all the weak lines could be measured, the problem of indexing a powder photograph of a triclinic crystal would be resolved first to the solving of the planar lattice given by equation (5), which contains only *three* constants A^*, B^* and γ to be determined. Once these constants are known, the application of equation (6) would yield the remaining two unknowns, α^* and β^*, and the problem would be solved.

Use of the density of the crystal

The density ρ of the crystalline powder can usually be accurately measured. The volume occupied by one molecule can then be calculated from

$$V_1 = 1{\cdot}6604M/\rho \quad \text{(in A.}^3\text{)},$$

or

$$V_1 = 1{\cdot}6502M/\rho \quad \text{(in kX.}^3\text{)},$$

where M is the molecular weight and V_1 is the volume per molecule. If there are n molecules per unit cell, the volume of the unit cell is $V_n = nV_1$.

Returning to the reciprocal space, we obtain for the reciprocal volume per molecule in A.$^{-3}$,

$$V_1^* = 1/V_1 = \rho/1{\cdot}66M, \tag{8}$$

and for the reciprocal volume of the unit cell:

$$V_n^* = V_1^*/n.$$

The value of V_1^* can usually be regarded as known, but the factor n, representing the number of molecules in the unit cell, which is a whole number, is unknown. The following equation can then be used with advantage:

$$V_n^* = a^*b^*c^* \sin\alpha^* \sin\beta^* \sin\gamma, \tag{9}$$

and, as c^* is known, this can be written as

$$V_1^*/c^* = nA^*B^* \sin\gamma. \tag{10}$$

The right-hand side of this equation has a simple meaning as the area of the unit cell of the planar lattice defined by equation (5), multiplied by the factor n.

If any two of the three constants A^*, B^*, γ are known, then equation (10) gives the third, when reasonable values of n are assumed. In the first step of the calculation, the solution of the problem of a triclinic crystal is reduced to a determination of only *two* constants, equivalent to the recognition of two heads of bands of lines on the photograph.

If only the head of the first band can be recognized, the method cannot be applied to a triclinic but it is still applicable to a monoclinic crystal, for which $\alpha = 90°$ and $\gamma = 90°$ so that equations (5), (6) and (10) are simplified into

$$H^{*2} = h^2A^{*2} + k^2B^{*2}, \tag{11}$$

$$L^* = lc^* + hA^* \cot\beta^*, \tag{12}$$

$$V_1^*/c^* = nA^*B^*. \tag{13}$$

However, sometimes even the head of the first band might not be recognized without ambiguity, but if one deals with a whole series of substances, known to be in the same modification, then it may be possible to decide which of the possible solutions is the most probable.

Use of the inter-edge angles of the crystals

Owing to the thinness of the crystals of the long-spacing compounds, as a rule, only the {001} faces are well developed, so that goniometric measurement of the *interfacial* angles is impracticable. Only the *inter-edge* angles on the periphery of the plate are accessible to measurement.

The crystals usually adhere with their {001} faces to the microscope slide, so that both the a and b crystallographic axes lie in the plane of the slide. If the interference figure can be seen, and if the crystal is monoclinic or orthorhombic, the directions of the a and b axes can then be determined, so that all the edge angles can be measured from the b cell-edge and in the (001) plane.

The edge indices will be enclosed in square brackets. Two crystal faces (hkl) and $(h'k'l')$ intersect in an edge having indices $[h''k''l'']$, given by

$$h'' = \begin{vmatrix} k & l \\ k' & l' \end{vmatrix}, \quad k'' = \begin{vmatrix} l & h \\ l' & h' \end{vmatrix}, \quad l'' = \begin{vmatrix} h & k \\ h' & k' \end{vmatrix}$$

(Zachariasen, 1945).

For a plate, one face of which is (001), any other face having indices (hkl) would form an edge having indices $[k\bar{h}0]$ independent of the index l of the plane. The (100) plane would thus form $[0\bar{1}0]$ edge, and the (010) plane, [100] edge.

Let $\phi_{[hk0]}$ be the inter-edge angle between [010] and $[hk0]$. Then, for a monoclinic crystal,

$$\tan\phi_{[hk0]} = ha/kb,$$

or, using relations (7),

$$\tan\phi_{[hk0]} = hB^*/kA^*.$$

The information obtained from the measurement of the inter-edge angles is thus complementary to the information from the density measurements, the former giving the ratio, the latter the product of the two lattice constants A^*, B^* of the reciprocal plane lattice (11).

Graphical application of the indexing method

Equations (4), (5) and (6) lend themselves to a geometrical representation, so that the indexing can be done most conveniently by graphical methods.

Two graphical methods have been devised; their application to the same soap powder pattern is shown in Figs. 1 and 2.

In the first method, shown in Fig. 1, it is necessary only to plot, preferably in Indian ink, on as large a scale as possible, all the observed reciprocal spacings in the form of concentric semicircles each of radius D^* and centre at the origin of rectangular co-ordinates with a horizontal X-axis and a vertical Y-axis. A separate straight strip of paper is then prepared (not shown in Fig. 1), along the edge of which is marked a series of equidistant lines spaced by c^* from each other. If this strip is moved over the graph, keeping it parallel to the X-axis, till its intersection with the Y-axis is at a distance H_{hk}^* from the origin, then a position can be found at which the marks on the strip coincide with all the circles belonging to the same band. By finding such a coincidence, the head of the band can be recognized and marked on the Y-axis. The coincidences

are marked in Fig. 1 by black dots; the corresponding Miller indices are marked above each dot.

The second graphical method, shown in Fig. 2, does not use a separate strip of paper for finding coincidences; instead of using the strip, the equidistant marks spaced by c^* from each other are marked on the X-axis of the graph. Each mark so obtained then serves as a centre of a complete set of concentric circles each of a radius D^*. Numerous intersections of the circles thus result. It can be easily proved that if a band H^*_{hk} exists, all the circles belonging to this band would intersect at a series of points all lying at a distance H^*_{hk} from the X-axis. In practice, owing to the repetition of the pattern of the form of numerous intersections of circles. In practice, it is more accurate than the first method, as the best point of intersection of a large set of circles all belonging to the same band can be found with considerably higher accuracy than the best-fitting position of the movable graduated strip. In addition, the scatter of the set of circles not exactly passing through their common point of intersection, owing to the errors of measurement, gives a good indication of the accuracy of the measurements.

There is, however, one disadvantage of the more condensed presentation of the second method, especially when a small scale is used: the diagram tends to be over-

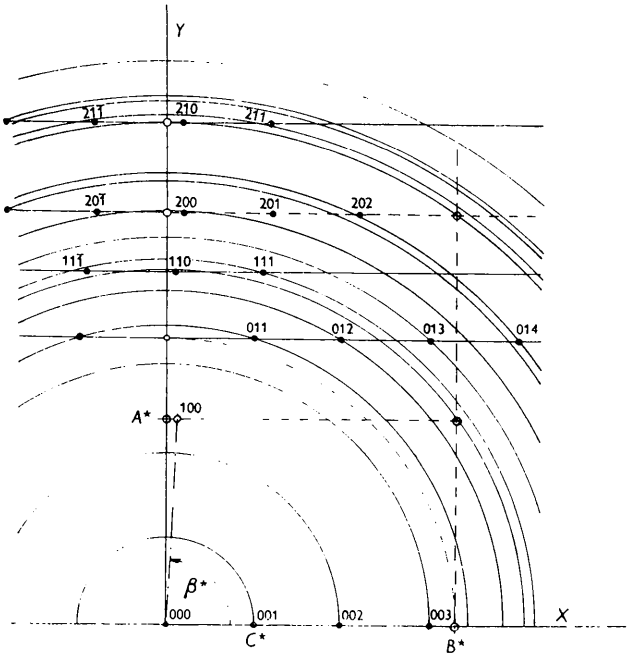

Fig. 1. Application of the first graphical method. Indexing of potassium caproate powder pattern.

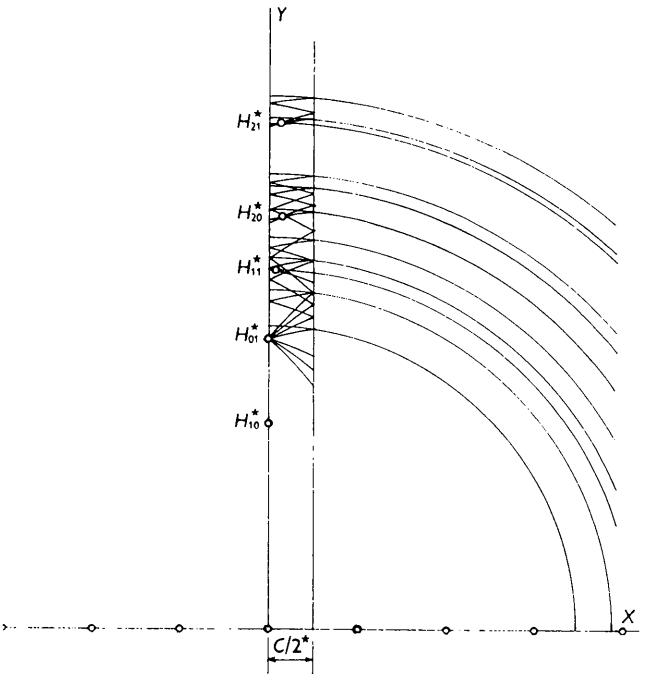

Fig. 2. Application of the second graphical method. Indexing of potassium caproate powder pattern.

the diagram along the X-axis with the identity period c^*, it is necessary to investigate only a narrow strip of the diagram running parallel to the Y-axis, the width of which is that of the identity period.

The width of this strip is further reduced to $\frac{1}{2}c^*$ owing to a line of symmetry parallel to the Y-axis and passing at a distance $\frac{1}{2}c^*$ from the origin. It is thus not necessary to draw full circles; only small arcs of each set of circles, which pass through the chosen strip, are required. (In Fig. 2, in order to prevent confusion on the scale of the figure, which is much smaller than is used in practice, many arcs of circles have been omitted.)

The second method has several advantages over the first method. It economizes paper, as only the narrow strip is to be preserved for reference. It records at once permanently all the possible solutions of the problem in crowded, so that the indexing of the lines is more difficult than in the first method.

Once the heads of the H^* bands are found by either method, the plane lattice (5) or (11) can be constructed in the following way (shown in Fig. 1 only).

When the head of a first band is located and the second band cannot be found by inspection, an attempt may be made to locate it by assuming that the crystal is monoclinic, and using equation (13). If two heads are located, equation (10) may be used to determine γ. Once the constants A^*, B^* and γ are determined, all the values of H^* can be found graphically by plotting (preferably in pencil, so that alterations may be made) on the same graph the plane lattice (5) or (11) and drawing circles with centre at the origin (shown in Fig. 1 as dashes) through its points till they intersect the Y-axis: these points may then be confirmed as heads of bands

either by applying the paper strip through them and observing coincidences with the Indian ink circles, or by finding intersections of the circles by the second method, till all the reflexions are accounted for.

Next comes the determination of the angles α^* and β^*. Two bands are chosen, preferably H^*_{10}, and H^*_{01}. In general, the choice of the angles α^* and β^* is not unique; in fact, any points on the first two independent bands can be chosen having index $l=0$. If one point of the band lies accurately on the Y-axis, it follows that the crystal cannot be triclinic, as α^* is a right angle. Otherwise the best practice is either to choose the strongest reflexion (which may lie some distance from the head of the band) or the reflexion nearest to the Y-axis, as having index $l=0$. The distance of this point from the Y-axis is then

$$L^*_{hk0}=hA^* \cot \beta^*+kB^* \cot \alpha^*, \qquad (14)$$

or for a monoclinic crystal

$$L^*_{hk0}=hA^* \cot \beta^*. \qquad (15)$$

If the crystal is triclinic, the two independent values of L^* give us two equations from which the two unknowns cot α^* and cot β^* can be obtained. Once these are fixed, distances L^*_{hk0} for all the other bands should be calculated and confirmed from the graph.

From the construction six constants are thus obtained which are c^*, A^*, B^*, γ, α^*, β^* arranged in the order as obtained.

From these, the constants of the unit cell can be calculated by means of the following equations:

$$a=1/(A^* \sin \gamma); \quad b=1/(B^* \sin \gamma);$$

$$\cos \gamma^*=\cos \alpha^* \cos \beta^*-\sin \alpha^* \sin \beta^* \cos \gamma, \qquad (16)$$

$$\cos \alpha=\frac{\cos \beta^* \cos \gamma^*-\cos \alpha^*}{\sin \beta^* \sin \gamma^*},$$

$$\cos \beta=\frac{\cos \alpha^* \cos \gamma^*-\cos \beta^*}{\sin \alpha^* \sin \gamma^*},$$

$$c=\frac{1}{c^* \sin \alpha \sin \beta^*}=\frac{1}{c^* \sin \alpha^* \sin \beta}.$$

Refinement of the lattice constants

If the measurements are of a high degree of accuracy, their accuracy may not be utilized to the full extent by the use of the graphical methods described, as any graphical method is necessarily limited in accuracy by the size of the graph that can be used in practice. It may thus be desirable to apply to the problems computing methods, which are not limited in accuracy, and to combine the measurements by the method of least squares. The equations (4), (5) and (6) are suitable for this purpose.

Let us assume that a sufficient number of lines in a given band was unequivocally identified and indexed and that their spacings were measured. In a band of constant Miller indices h and k, H^*_{kh} is constant. We can write equation (4) as follows:

$$D^{*2}_{hkl}=H^{*2}_{hk}+K^{*2}_{hk}+2K^*_{hk}lc^*+l^2c^{*2},$$

where $$K^*_{hk}=hA^* \cot \beta^*+kB^* \cot \alpha^*$$

is also constant for a given band.

Let us write

$$(D^*_{hkl}/c^*)^2-l^2=y_i, \quad l=x_i,$$

$$(H^*_{hk}/c^*)^2+(K^*_{hk}/c^*)^2=q, \quad \text{and} \quad 2K^*_{hk}/c^*=p.$$

We thus obtain n linear equations

$$y_i=px_i+q, \quad i=1, 2, \ldots, n,$$

where x_i are whole numbers, y_i are known from measurement, and p, q are two constants to be determined.

In order to determine p, q with highest possible accuracy any of the methods of calculation of the constants in a linear law can be used. If the Gaussian method of least squares is used, then, assuming that all the equations have equal weight,

$$p=P/U, \qquad q=Q/U,$$

where

$$P=n\Sigma x_iy_i-\Sigma x_i \Sigma y_i, \quad Q=\Sigma x_i^2 \Sigma y_i-\Sigma x_i \Sigma x_iy_i,$$

$$U=n \Sigma x_i^2-(\Sigma x_i)^2.$$

The probable errors in the values of p and q are then

$$\alpha_p=0{\cdot}6745 \{n\Sigma\delta_i^2/(n-2)\ U\}^{\frac{1}{2}},$$

$$\alpha_q=0{\cdot}6745 \{\Sigma x_i^2\ \Sigma\delta_i^2/(n-2)\ U\}^{\frac{1}{2}},$$

where $$\delta_i=y'_i-y_i,$$

and where y'_i are values calculated from the equation $y'_i=px_i+q$, by using the calculated values of p and q. The formulae do not apply to equations having unequal weights.

Once p, q are determined, we can calculate H^*, K^* from

$$H^*_{hk}=c^* (q-\tfrac{1}{4}p^2)^{\frac{1}{2}} \quad \text{and} \quad K^*_{hk}=\tfrac{1}{2}pc^*.$$

The calculation of the other lattice constants can then proceed on the same lines as described in previous paragraphs, i.e. H^*_{10} gives A^*, H^*_{01} gives B^*, H^*_{11} gives γ, K^*_{10} and K^*_{01} give then β^* and α^*, etc., so that the best values of all the parameters of the unit cell may be obtained together with their probable errors. This method of least squares is not limited to powder photographs; it can be used for measurement of single crystal photographs if required. It has been successfully used in determining accurate values of the unit cell of potassium caprate ($KC_{10}H_{19}O_2$) from its powder photograph and single crystal photographs, details of which will be published elsewhere (Vand, Lomer & Lang, 1947).

Example of the application of the graphical method

As an example of the application of the graphical method the unit cell of potassium caproate ($KC_6H_{11}O_2$) is derived from its powder pattern. This soap has been

chosen for its comparatively small value of the long spacing $c \sin \beta$ (= 18·89 kX.), so that the Figs. 1 and 2, reproduced on a small scale, are not unduly overcrowded. This, on the other hand, has a disadvantage that the 'heads' of the bands are much more spread out than in other cases, so that they are rather more difficult to detect on first inspection than in compounds with really large long spacings.

The structure of potassium caproate has not yet been described; we found that there exist several crystalline forms of potassium soaps and that the potassium caproate investigated belongs to a form provisionally labelled as *A*.

The powder pattern was obtained by Lomer (unpublished work) with a 12·5 cm. focusing camera, using Cu $K\alpha$ nickel-filtered radiation. The measurements are given in Table 1. Relative intensities of the lines are expressed on a scale of the strongest short spacing line taken as 100, and are given in the first column. In the second column are given values of n/d expressed in kX.$^{-1}$ In the third column are given the indices of the lines, obtained by the graphical indexing methods, as described.

Table 1. *Powder diffraction pattern of potassium caproate (form* A)

Relative intensity	n/d	Index	Relative intensity	n/d	Index
200	0·0528	001	1	0·4102	†
1	0·1052	002	1	0·4242	†
1	0·1596	003	2	0·4340	†
3	0·1825	011	5D	0·4432	†
3	0·2036	012	2	0·4560	†
40D	{0·2166 / 0·2222}	110†	5	0·4617	†
10	0·2361	013	2	0·4774	†
30	0·2512	200	2	0·4827	†
30	0·2694	$20\bar{2}$	10	0·5023	400†
2	0·2745	014, 202	5	0·5108	$40\bar{2}$†
100	0·3047	210	1	0·5340	†
80	0·3096	211, $21\bar{1}$	3	0·5479	†
1	0·3177	015	3	0·5657	†
40	0·3202	$21\bar{2}$	1	0·5880	†
1	0·3423	$21\bar{3}$	1	0·6006	†
1	0·3492	020	2	0·6129	†
3	0·3535	021	2	0·6989	†
3	0·3643	†	—	—	—
1	0·3713	†	—	—	—
1	0·4006	†	—	—	—

D = Diffuse.

† There are more than two possible ways of indexing these reflexions.

The following data were used:

Molecular weight	$M = 154{\cdot}16$
Observed density	$\rho = 1{\cdot}182$ g.cm.$^{-3}$
Reciprocal volume occupied by one molecule	$V_1^* = 4{\cdot}646 \times 10^{-3}$ kX.$^{-3}$
Reciprocal long spacing	$c^* = 0{\cdot}05293$ kX.$^{-1}$
Reciprocal area of the unit cell of the planar lattice per single molecule	$V_1^*/c^* = 0{\cdot}0887$ kX.$^{-2}$

Inter-edge angles could not be measured.

By applying the first and the second graphical method, as shown on Figs. 1 and 2, the crystal was found to be probably monoclinic, with $A^* = 0{\cdot}1254$ kX.$^{-1}$ and $B^* = 0{\cdot}1744$ kX.$^{-1}$ Assuming $n = 4$ molecules per unit cell, $nA^*B^* = 0{\cdot}0875$, which is in good agreement with the value of V_1^*/c^* calculated from the density.

Taking for the (200) reflexion that which gives the angle β nearest to 90°, $\beta = 92°$ is obtained. This gives us the following values of the unit cell:

$$a = 7{\cdot}97 \text{ kX.}, \quad b = 5{\cdot}73 \text{ kX.}, \quad \beta = 92°,$$

$$c \sin \beta = 18{\cdot}89 \text{ kX.}, \quad c = 18{\cdot}90 \text{ kX.}$$

It should be noted that the whole (10*l*) band is probably missing, and in addition the (010) reflexion of the (01*l*) band is probably missing. There is a tentative indication of a glide plane and a screw axis, but the determination of the space group is not possible from the above data given by powder photographs. The (11*l*) band is diffuse.

Conclusions

The method described is not as certain as single crystal methods, mainly for the following reasons:

1. In a powder photograph many reflexions escape detection, whereas they could be easily registered on a single crystal photograph. Such reflexions may be vital for deciding the dimensions of the unit cell, and especially the symmetry and space group of the crystal.

2. Even if the chemical purity of the samples is guaranteed, the modification under investigation may be contaminated by the presence of another modification of the same substance, giving rise to additional diffraction rings. Such rings may be very confusing when using the method described, whereas this difficulty rarely arises in single crystal work.

3. Even if a sufficiently numerous series of substances differing in chain length is available, it is not certain, *a priori*, that the series is all in the same crystalline modification. A useful criterion is to investigate the long spacings and the densities; if the long spacings do not form a linear function of the chain length and the areas V_1^*/c^* are not constant, there are different modifications present.

4. If the *c*-edge is too short it may be difficult to recognize the bands on the graph without ambiguity, and there may even be difficulties in recognizing c^*. On the other hand, if the *c*-edge is too long, the individual bands may become unresolvable by the camera.

Owing to these limitations, the indexing method for powder photographs here described should not be regarded as an equivalent to a single crystal method, but only as an alternative when single crystals are not available. However, in spite of its limitations, the

method has been applied with success to homologous series of sodium, potassium, lithium and silver soaps containing from four to twenty carbon atoms in the hydrocarbon chains.

I wish to thank Mr A. Lang for the preparation of the potassium caproate and Mr T. R. Lomer for measurement of the photographs, and the Directors of Lever Brothers and Unilever Limited for permission to publish this paper.

References

VAND, V., LOMER, T. R. & LANG, A. (1947). *Nature, Lond.*, **159**, 507.

ZACHARIASEN, W. H. (1945). *Theory of X-ray Diffraction in Crystals*. New York: Wiley.

Acta Cryst. (1948). **1**, 115

Die Kristallstruktur des einwertigen Kupferazids, CuN_3

VON HEINZ WILSDORF

Institut für allgemeine Metallkunde, Göttingen, Deutschland

(*Eingegangen* 15 *Januar* 1948)

CuN_3 belongs to the space group C_{4h}^6–$I4_1/a$ with cell dimensions $a = 8{\cdot}65_3 \pm 0{\cdot}01$ A., $c = 5{\cdot}59_4 \pm 0{\cdot}01$ A., $c/a = 0{\cdot}646$. The observed density is 3·26 g.cm.$^{-3}$, giving $Z = 8$ and a calculated density of 3·34 g.cm.$^{-3}$ The atomic positions are: 8 Cu at (*d*); 8 N_I at (*c*); and 16 N_{II} at (*f*) with parameters $x = 0{\cdot}077$, $y = 0{\cdot}173$, $z = 0{\cdot}250$. The structure consists of Cu ions and of N_3 groups which are arranged in chains in the direction of the body diagonal of the cell. The structure is not related to any known standard type.

Während die strukturell bekannten anorganischen Azide nur als ein- oder zweiwertige Verbindungen vorkommen, bildet die Stickstoffwasserstoffsäure mit Kupfer das Monoazid CuN_3 und das Diazid $Cu(N_3)_2$. Somit ist ein Vergleich von Strukturen mit einer oder zwei N_3-Ketten bei dem gleichen Metall möglich. Als erster Teil der Untersuchung soll in dieser Arbeit die Struktur des CuN_3 beschrieben werden.

Die Darstellung des CuN_3 wurde zunächst durch Wöhler & Krupko (1913) und Martin (1915) bekannt. Sie reduzierten eine Kupfersulfatlösung mit Kaliumbisulfit, gaben sie zu Natriumazid und beobachteten einen feinen weissen Niederschlag (Verfahren I). Bei eigenen Versuchen nach diesem Verfahren konnten Kristallnadeln bis zu 3 mm. Länge erhalten werden, die röntgenographisch nach dem Drehkristallverfahren untersucht wurden. Die Aufnahmen ergaben tetragonale Symmetrie mit $a = 8{,}64$ A. und $c = 5{,}60$ A. Eine zweite Möglichkeit der Darstellung wurde von Straumanis & Cirulis (1943) beschrieben. Danach lässt man wässrige HN_3 auf Kupferpulver einwirken, das nach mehreren Tagen in eine farblose Substanz übergeht (Verfahren II), die dieselben Interferenzen wie die nach Verfahren I dargestellten Kristalle zeigte. Aus den unregelmässigen Aggregaten konnten keine Einkristalle isoliert werden.

Für die genaue Bestimmung der Gitterkonstanten (nach Straumanis) wurde ein Präparat nach Verfahren II gewählt, das $a = 8{,}65_3 \pm 0{,}01$ A. und $c = 5{,}59_4 \pm 0{,}01$ A. ergibt; $c/a = 0{,}646$. Die pyknometrisch bestimmte Dichte beträgt $\rho = 3{,}26$ g.cm.$^{-3}$ ($\rho_{\text{röntg.}} = 3{,}34$ g.cm.$^{-3}$); die Zelle enthält danach 8 Moleküle: 8 Kupfer- und 24 Stickstoffatome. Da in den bekannten Aziden immer drei Stickstoffatome eine Kette bilden, wird das Gleiche auch hier als Arbeitshypothese zur Ermittlung der Struktur benutzt.

Die Flächenstatistik führt auf ein raumzentriertes Gitter. Die beobachteten Auslöschungen sind charakteristisch für die Raumgruppen C_{4h}^6–$I4_1/a$ und D_{4h}^{19}–$I4/amd$; möglich sind ferner alle Raumgruppen der Klassen C_{4h}–$4/m$, C_4–4, S_4–$\bar{4}$, sowie $D_{4h}^{1,4,6,7,9,12,14,17,19}$, D_4^{1-10}, $C_{4v}^{1,4,6,7,9,12}$ und $D_{2d}^{1-5,8,9,11,12}$.

Da zwischen D_{4h}^{19}–$I4/amd$ und C_{4h}^6–$I4_1/a$ nicht experimentell entschieden werden konnte,* wurde die Ausschliessung auf rechnerischem Wege vorgenommen. Die beiden Raumgruppen unterscheiden sich durch die 16- und 32-zähligen Punktlagen. Wie bei der Diskussion von C_{4h}^6–$I4_1/a$ später gezeigt werden wird, können die 16 äusseren Stickstoffatome nicht in den den beiden Raumgruppen gemeinsamen 4- und 8-zähligen Lagen untergebracht werden. Ferner ergab die Intensitätsrechnung, dass mit den bei D_{4h}^{19}–$I4/amd$ angegebenen 16-zähligen Lagen, bei denen die Ketten nur senkrecht zur *c*-Achse liegen können, die beobachteten Intensitäten in keiner Weise wiedergegeben werden. Da ferner bei D_{4h}^{19}–$I4/amd$ nur noch eine 32-zählige Punktlage zur Verfügung steht, kann diese Raumgruppe für die Struktur nicht in Frage kommen.

Die zweite wahrscheinliche Raumgruppe ist C_{4h}^6–$I4_1/a$. Hier stehen 4-, 8- und 16-zählige Punktlagen zur

* Aus äusseren Gründen waren Schwenk- oder Goniometeraufnahmen nicht möglich.